

Adaptive Reactive Power Control of PV Power Plants for Improved Power Transfer Capability under Ultra-Weak Grid Conditions

Dongsheng Yang, *Member, IEEE*, Xiongfei Wang, *Member, IEEE*, Fangcheng Liu, Kai Xin, Yunfeng Liu, Frede Blaabjerg, *Fellow, IEEE*

Abstract—This paper analyzes the power transfer limitation of the PV power plant under the ultra-weak grid condition, i.e., when the Short-Circuit Ratio (SCR) is close to 1. It explicitly identifies that a minimum SCR of 2 is required for the PV power plant to deliver the rated active power when operating with the unity power factor. Then, considering the reactive power compensation from PV inverters, the minimum SCR in respect to Power Factor (PF) is derived, and the optimized coordination of the active and reactive power is exploited. It is revealed that the power transfer capability of PV power plant under the ultra-weak grid is significantly improved with the low PF operation. An adaptive reactive power droop control is next proposed to effectively distribute the reactive power demands to the individual inverters, and meanwhile maximize the power transfer capacity of the PV power plant. Simulation results of a 200 MW PV power plant demonstrate that the proposed method can ensure the rated power transfer of PV power plant with the SCR of 1.25, provided that the PV inverters are operated with the minimal $PF=0.9$.

Index Terms—Photovoltaic power systems, Reactive power compensation, Droop control, Power transmission.

I. INTRODUCTION

Benefiting from the significant technical advances in solar cells and power electronics, the costs of the utility-scale Photovoltaic (PV) power plants have become competitive with other intermittent renewable power sources [1]-[2]. Large scale PV power plants have been increasingly installed worldwide, and the accumulative global utility-scale PV capacity is heading towards 100 GW [3]. Due to the low energy densities and uneven distributions of solar resources, these PV power plants are deployed in remote areas or even desert with high solar irradiance [4]. As a consequence, the long-distance power transmission lines with low Short-Circuit-Ratio (SCR) have become the major bottleneck to effectively transmit the generated power to the load center [5]-[6].

To unblock the bottleneck caused by the high-impedance grids, power-electronic-based power transmission technology based on the High Voltage Direct Current (HVDC) system [7], and Flexible Alternative Current Transmission Systems (FACTS) devices, have recently been used to improve the power transfer capability [8]. However,

these solid-state power electronic equipment are featured with low inertia and fast dynamics. A wide frequency range of dynamic interactions among the HVDC systems, FACTS devices and grid-connected inverters of renewable energy sources pose new challenges to the system stability and power quality [9-12]. It hence becomes more appealing to utilize the power controllability of PV inverters for increasing the power transfer capacity under weak grid conditions, which is also more advantageous by sharply cutting down the cost of upgrading grid infrastructure.

The PV power plant can be controlled as FACTS devices [13], which provides a cost-effective solution to damp the sub-synchronous oscillations [14] and improve transient stability of the power system [15]. The prerequisite of these control functions is that the excessive power capacity is available from the PV inverters. However, under the ultra-weak grid condition, i.e., the SCR of the grid is close to 1, the available power capacity must be utilized to provide internal reactive power support, because delivering the rated active power could already be a great challenge for the PV power plant. Similar scenarios have been reported in the VSC-HVDC system [16], and the power limitations imposed by both the magnitude and the phase angle of the transmission line have been investigated. This problem could be more complicated when it comes to the PV power plant, as PV inverters usually are operated with the limited PF typically ranging within $\pm 0.9/0.95$ [17]-[18]. Moreover, the huge number of the PV inverters that are distributed over a vast area within the power plant further increases the difficulty of the power control.

Many research works have been reported on the flexible power control methods for distributed PV inverters. Basically, they can be grouped as centralized control [19]-[21] and decentralized control [22]-[23]. As for the centralized control, a communication network among a great number of distributed inverters must be established. This incurs additional costs and may introduce communication reliability problems. On the contrary, the decentralized controls can achieve automatic power regulation based on the local information. To alleviate the voltage variation caused by injection of the fluctuated power, the PV inverter can regulate its reactive power according to the local voltage and local active power production [24]-[27]. These control methods are usually developed for the PV inverters connected to the low voltage distribution networks, aiming to address the voltage fluctuations caused by the intermittent solar power flowed through the line impedance with a high R/X ratio [28]. The decentralized power controllers need to be carefully tuned to reach a compromise between the sufficient voltage support and the unnecessary reactive power consumption or generation [29].

Despite varieties of power controls have been extensively

Manuscript received May 26, 2017; revised July 11, 2017; accepted September 29, 2017. This work was supported in part by the European Research Council (ERC) under the European Union's Seventh Framework Program (FP/20072013)/ERC Grant Agreement 321149-Harmony; and also by VILLUM FONDEN under the VILLUM Investigators Grant-REPEPS. D. Yang, X. Wang and F. Blaabjerg are with the Department of Energy Technology, Aalborg University, Aalborg, DK-9220 Denmark (e-mail: doy@et.aau.dk; xwa@et.aau.dk; fbl@et.aau.dk), and F. Liu, K. Xin, Y. Liu are with Watt Lab, Central Research Institute of Huawei Technologies Co., LTD. Shanghai, 201206, China (e-mail: formula.liu@huawei.com, kai.xin@huawei.com, yf.liu@huawei.com)

investigated, the research scopes are mainly focused on the mitigation of voltage fluctuations at multiple nodes of low-voltage distribution networks [30]-[31]. As for the PV power plant under the ultra weak grid condition, the consumed reactive power on the transmission line can exceed half of the power rating of the whole PV plant. In this case, the major challenge for the PV plant lies in the limitation of power transfer capability rather than the power quality issues. In the other words, it is necessary to coordinate the active and reactive power of PV power plants to maximize its power transfer capacity, and thus to alleviate the requirement of oversizing PV inverters or installing additional expensive FACTS devices. To the best knowledge of the authors, this topic has remained unaddressed in the scientific literature. The present paper attempts to fill in this gap and the main contribution of this paper can be summarized as 1) Quantifying the relationship between the SCR and the *PF* of PV inverters for transferring the rated active power. 2) Coordination of the active power and reactive power to maximize the power transfer capacity. 3) An adaptive reactive power control method is proposed for PV power plant to automatically dispatch the reactive power demands on the individual inverters and meanwhile achieves the optimal power coordination control. In this way, the power transfer capacity of the PV power plant can be improved to the theoretical limit. Additionally, the voltage variation at the Point of Common Coupling (PCC) caused by the active power injection can be dynamically compensated.

II. POWER LIMITATION OF PV POWER PLANT OPERATED UNDER UNITY POWER FACTOR

Fig. 1 shows a typical configuration of the PV power plant. It contains numerous generation units and each unit contains a DC/DC converter for local maximum power point tracking (MPPT) control and a DC/AC inverter for grid-connections. All the generation units are connected to the PCC through low-voltage power cables and then fed into the high-voltage transmission network through the substation. To minimize the power loss on the low-voltage cable, the generation units are distributed evenly around the substation in order to minimize the length of the low-voltage cables.

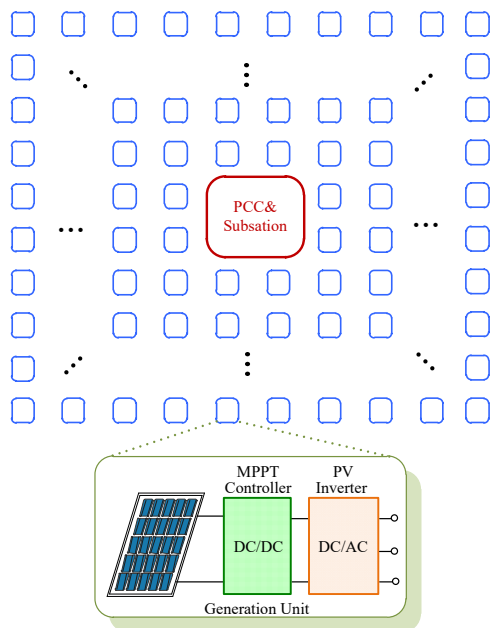


Fig. 1. The configuration of a PV power plant.

The PV inverters are usually current-controlled to improve the power quality, so the whole farm can be treated as an ideal current source at the fundamental frequency. Meanwhile, the grid can be represented by its Thevenin equivalent circuit. Therefore, the simplified circuit of the whole grid-connection system can be obtained, as shown in Fig. 2, where i_{pv} is the grid current injected by PV power plant, v_{pcc} is the voltage at PCC, v_g and Z_g are the equivalent grid voltage and grid impedance at the PCC. Here, a resistor R_g and a series inductance X_g are used to model the grid impedance Z_g that is introduced by a long transmission line and a step-up power transformer.

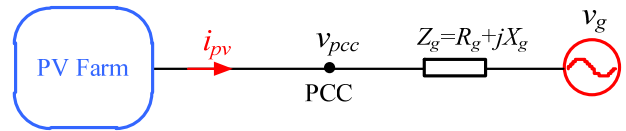


Fig. 2. The equivalent circuit of grid connection system.

The stiffness of the grid at the PCC can be depicted by the SCR, which can be expressed as [15]:

$$SCR = \frac{P_{SC}}{P_{pv_rated}} \triangleq \frac{V_g^2 / |Z_g|}{P_{pv_rated}} \quad (1)$$

where P_{SC} is the short circuit power of the grid at the PCC, expressed as $P_{SC} \triangleq V_g^2 / |Z_g|$, and P_{pv_rated} is the rated generation power of the whole PV plant.

Accordingly, $|Z_g|$ can be represented by the SCR, which is expressed as:

$$|Z_g| = \frac{V_g^2}{P_{pv_rated} \cdot SCR} \quad (2)$$

When the PV power plant is operated under the unity PF condition, the phasor diagrams are shown in Fig. 3, where \dot{I}_{pv} , \dot{V}_{pcc} and \dot{V}_g are the phasors of i_{pv} , v_{pcc} and v_g , respectively.

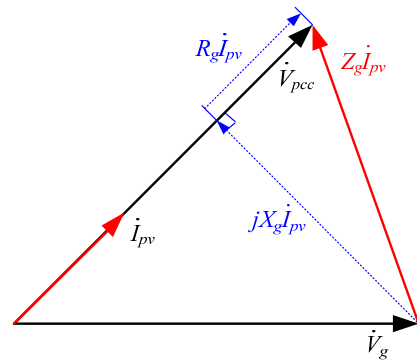


Fig. 3. Phasor diagrams when PV power plant is operated with unity PF.

From Fig. 3, the root-mean-square (RMS) value of v_{pcc} can be derived as:

$$V_{pcc} = \sqrt{V_g^2 - (X_g \cdot I_{pv})^2} + R_g \cdot I_{pv} \quad (3)$$

where I_{pv} is the RMS value of i_{pv} . The active power injected by the PV power plant is given by:

$$P_{pv} = V_{pcc} \cdot I_{pv} \quad (4)$$

According to (2) and (3), the curves of V_{pcc} vs. I_{pv} and P_{pv} vs. I_{pv} under different R_g/X_g ratios when $SCR=1$ can be obtained, as shown in Figs. 4 and 5, respectively. As seen,

V_{pcc} drops significantly at the rated I_{pv} injection, especially under the low R_g/X_g ratio. Correspondingly, the active power injected by PV power plant P_{pv} is also greatly limited. According to (2)-(4), the maximal of P_{pv} can be derived as:

$$P_{pv_max} = \frac{1}{2} \cdot \frac{1}{1 - \frac{1}{\sqrt{1 + (X_g/R_g)^2}}} \cdot \frac{V_g^2}{|Z_g|} \quad (5)$$

In order to deliver the rated power into the grid, i.e., $P_{pv_max} > P_{pv_rated}$, the minimum SCR is required, and its expression can be derived based on (2) and (5), which is given by:

$$SCR_{min} = 2 - \frac{2}{\sqrt{1 + \frac{1}{(R_g/X_g)^2}}} \quad (6)$$

It can be seen that the PV power plant can operate under a lower SCR when the R_g/X_g ratio of the grid impedance is increased. However, since the PV power plant is usually fed into the high voltage transmission network with low R_g/X_g ratio, the power limitation is more severe. Based on (6), a minimum SCR of 2 can be identified when the R_g/X_g ratio approaches to 0.

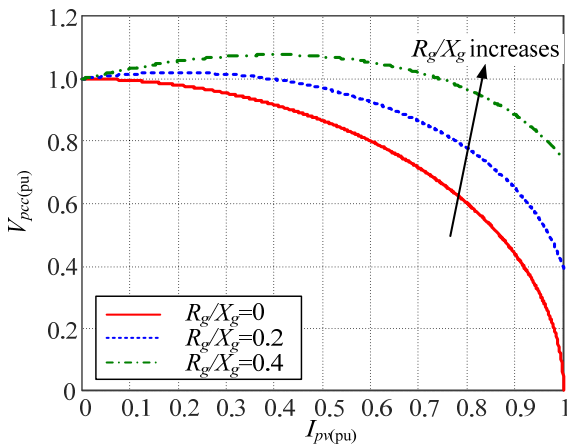


Fig. 4. Curves of V_{pcc} vs. I_{pv} under different R_g/X_g ratios when $SCR=1$.

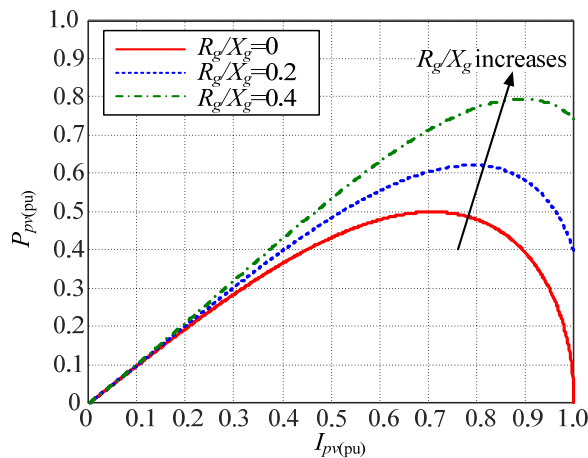


Fig. 5. Curves of P_{pv} vs. I_{pv} under different R_g/X_g ratios when $SCR=1$.

III. POWER LIMITATION OF PV POWER PLANT OPERATED UNDER VARIABLE POWER FACTOR

In order to operate PV power plant under the ultra-weak grid condition, the common practice is to reshape the system

impedance using locally installed bulk FACTS devices, of which the operational principle is to provide the necessary reactive power to compensate/cancel the voltage drop of the original transmission line. However, to reshape the system impedance under the ultra weak grid condition, the required reactive power from FACTS device can be considerably high which makes the installation of FACTS device costly. Alternatively, the required reactive power can also be provided by the PV inverters themselves.

Take $Q = 0.5P_{rated}$ as the example, the FACTS device with the power rating of $0.5P_{rated}$ has to be installed for the external reactive power compensation. However, PV inverters with the power rating of $\sqrt{1+0.5^2}P_{rated} = 1.118P_{rated}$, are able to provide the same amount of reactive power with the rated active power output, which is more cost-effective. In this case, the PV power plant has to operate with variable PF , and its power limitation will be further discussed. Here, the grid impedance is assumed to be purely inductive to draw the worst case, i.e., $Z_g=jX_g$.

Fig. 6 shows the phasor diagrams of the PV power plant and the grid with different phase angle φ , for different PF . $I_d = I_{pv} \cos \varphi$ is the d -axis current component which is in phase with \dot{V}_{pcc} , and $I_q = I_{pv} \sin \varphi$ is the q -axis current component which is vertical to \dot{V}_{pcc} .

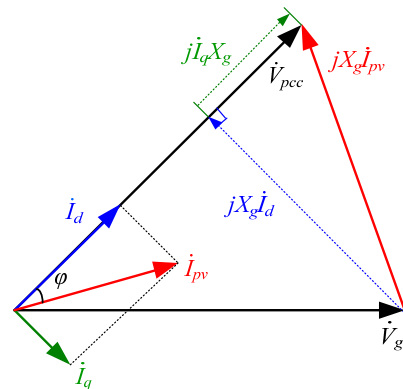


Fig. 6. Phasor diagrams using distributed reactive power compensation

According to Fig. 6, the output active power is given by:

$$\begin{aligned} P_{pv} &= V_{pcc} \cdot I_d \\ &= \left(\sqrt{V_g^2 - (X_g \cdot I_d)^2} + X_g \cdot I_q \right) \cdot I_d \\ &= \left(\sqrt{V_g^2 - (X_g \cdot I_{pv} \cos \varphi)^2} + X_g \cdot I_{pv} \sin \varphi \right) \cdot I_{pv} \cos \varphi \end{aligned} \quad (7)$$

In order to deliver the rated power to the grid, i.e., $P_{pv} > P_{pv_rated}$, the following inequality should be satisfied:

$$\left(\sqrt{1 - \left(\frac{X_g}{V_g} \cdot I_{pv} \cos \varphi \right)^2} + \frac{X_g}{V_g} \cdot I_{pv} \sin \varphi \right) \cdot \frac{I_{pv} \cos \varphi}{I_{pv_rated}} \geq 1 \quad (8)$$

Considering $Z_g=jX_g$, (2) can be rewritten as:

$$\frac{X_g}{V_g} = \frac{V_g}{P_{pv_rated} \cdot SCR} = \frac{1}{I_{pv_rated} \cdot SCR} \quad (9)$$

Substituting (9) into (8), yielding:

$$\left[\sqrt{1 - \left(\frac{I_{pv(pu)} \cos \varphi}{SCR} \right)^2} + \frac{I_{pv(pu)} \sin \varphi}{SCR} \right] \cdot I_{pv(pu)} \cos \varphi \geq 1 \quad (10)$$

where $I_{pv(pu)}=I_{pv}/I_{pv_rated}$ is the per unit value of injected grid current. Therefore, the minimum SCR with respect to $I_{pv(pu)}$ and φ can be derived as:

$$SCR_{min} = \frac{I_{pv(pu)}^2 \sin \varphi \cos \varphi - (I_{pv(pu)} \cos \varphi)^2 \sqrt{I_{pv(pu)}^2 - 1}}{1 - (I_{pv(pu)} \cos \varphi)^2} \quad (11)$$

Considering $\varphi=\arccos(PF)$, the curves of SCR_{min} vs $I_{pv(pu)}$ under different PFs can be drawn as shown in Fig. 7. The PV power plant can be operated under a lower SCR as the PF reduces. Therefore, a minimum of 0.9 PF can be preserved for PV power plant to operate under the ultra-weak grid condition with SCR close to 1.

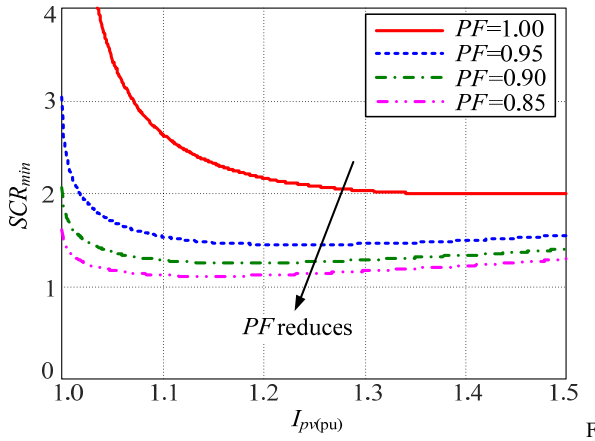


fig. 7. SCR_{min} curves vs $I_{pv(pu)}$ under different PFs

$$\varphi \leq \arcsin \left(\frac{I_{pv(pu)}^2 + SCR^2 (k^2 - 1)}{2 I_{pv(pu)} \cdot SCR \cdot k} \right) \quad (16)$$

Therefore, according to (12), (13) and (16), the $I_{pv(pu)}_{min}$ curves with respect to PF under different SCRs can be depicted by Fig. 8, where $k=1.05$. From Fig. 8, the conclusion can be drawn that the reactive power should be produced as much as possible until the PCC voltage achieves its limits. In this way, the current rating of the PV inverters can be reduced at rated active power injection, which helps to improve the efficiency and alleviates the requirement of oversizing PV inverters.

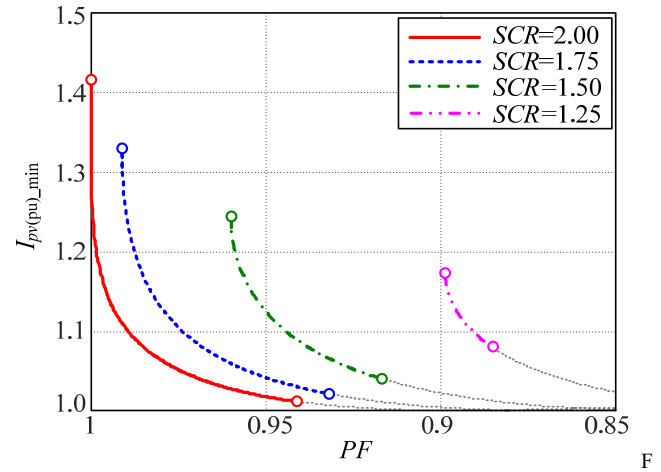


fig. 8. $I_{pv(pu)}_{min}$ curves vs PF under different SCRs

IV. COORDINATION OF ACTIVE POWER AND REACTIVE POWER OF PV PLANTS

For a given SCR condition, it is desirable to reduce the current rating of PV inverters when transferring the same rated active power. Or, put it in another way, to maximize transfer capability of active power given the same current rating. Moreover, practical constraint from PCC voltage should also be taken into consideration. So the coordination of active power and reactive power is mandatory.

To better address this issue, the minimum $I_{pv(pu)}$ in respect to φ and SCR can be derived according to (10), which is expressed as:

$$I_{pv(pu)}_{min} = \sqrt{\frac{(2 \tan \varphi SCR + SCR^2) - \sqrt{(2 \tan \varphi SCR + SCR^2)^2 - 4 \frac{SCR^2}{\cos^2 \varphi}}}{2}} \quad (12)$$

where φ should satisfy:

$$\varphi \geq 2 \arctan \left(\frac{2 - SCR}{2 + SCR} \right) \quad (13)$$

Otherwise, it is impossible to deliver the rated power into the grid. Moreover, another constraint on the power factor angle φ results from the limitation of the PCC voltage. Assuming that $V_{pcc} < k V_g$, where k is voltage limitation coefficient, then,

$$V_{pcc} = \sqrt{V_g^2 - (X_g I_{pv} \cos \varphi)^2} + X_g I_{pv} \sin \varphi \leq k V_g \quad (14)$$

Dividing V_g at both sides of the inequality (14), yields:

$$\sqrt{1 - \left(\frac{I_{pv(pu)} \cos \varphi}{SCR} \right)^2} + \frac{I_{pv(pu)} \sin \varphi}{SCR} \leq k \quad (15)$$

The power factor angle φ should satisfy:

V. ADAPTIVE REACTIVE POWER CONTROL OF PV POWER PLANTS

To properly distribute the reactive power demand among the individual inverters, all the inverters can regulate its reactive power according to the droop control scheme, as shown in Fig. 9(a). It means that the PCC voltage has to be intentionally reduced when required reactive power is increased, such that individual inverters can increase their reactive power simultaneously according to the reduction of PCC voltage. In order to equally share the reactive power, the droop controllers of inverters are tuned the same droop coefficient. The output reactive power of each inverter is given by:

$$Q = (V_n - V_{pcc}) \frac{Q_{max}}{\Delta V_{max}} \quad (17)$$

where V_n is the nominal value of V_{pcc} , ΔV_{max} and Q_{max} are the maximum droop voltage and the output reactive power, respectively.

Since terminal voltage of individual PV inverters can be slightly different from each other due to the voltage drops on the low-voltage cables, a detectable value of ΔV_{max} must be guaranteed in order to ensure the good reactive power sharing among different inverters. Usually, ΔV_{max} is set to 5%~10% of V_n . As a result, V_{pcc} will inevitably fall below its nominal value when the PV power plant injects the active power, so the inverter's current rating has to be increased in order to inject the same rated active power. In other words, the power transfer capability of the PV power plant is reduced due to the voltage drop at PCC, given the same inverter's current rating.

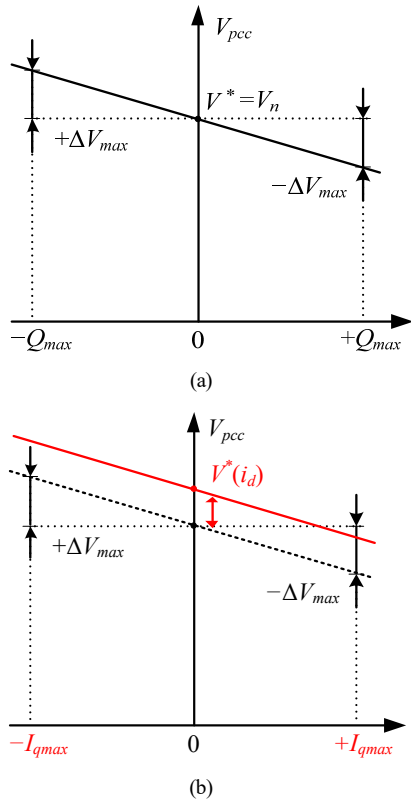


Fig. 9. Distributed reactive power control method (a) Conventional droop control (b) Proposed adaptive droop control

In order to minimize the V_{pcc} variation, V^* can be regulated dynamically to restore V_{pcc} to its nominal value. Since V_{pcc} variation is mainly caused by the injected reactive power of PV power plant, an adaptive law is proposed to adjust V^* dynamically and thus to minimize the variation of the PCC voltage V_{pcc} . The control scheme of this adaptive droop control is shown in Fig 9(b), where I_{qmax} is the available output q -axis current at rated reactive power rejection limited by a minimal PF_{min} , given by:

$$I_{qmax} = \frac{P_n}{V_n} \frac{\sqrt{1 - PF_{min}^2}}{PF_{min}} \quad (18)$$

The output q -axis current i_q is given by:

$$i_q = (V^*(i_d) - V_{pcc}) \cdot D_{iq} \quad (19)$$

where $D_{iq} = I_{qmax} / \Delta V_{max}$ is the droop coefficient of q -axis current.

According to Fig. 6, the desirable compensated voltage at PCC ΔV_{com} can be predicted given that I_d is known, which is expressed by:

$$\begin{aligned} \Delta V_{com} &= I_q X_g = V_n - \sqrt{V_g^2 - (X_g I_d)^2} \\ &\approx V_n - \sqrt{V_n^2 - (X_g I_d)^2} \end{aligned} \quad (20)$$

Accordingly, the required reactive current is given by:

$$I_q = \frac{\Delta V_{com}}{X_g} = \frac{V_n}{X_g} - \sqrt{\left(\frac{V_n}{X_g}\right)^2 - I_d^2} \quad (21)$$

Referring to (19), this reactive current can be automatically provided by adjusting the V^* with respect to i_d , and the adaptive law for each inverter can be derived as:

$$V^*(i_d) = V_n + \Delta V(i_d) \quad (22)$$

where $\Delta V(i_d)$ is expressed by:

$$\Delta V(i_d) = \frac{I_q}{N} \cdot \frac{1}{D_{iq}} = \frac{V_n}{D_{iq} N X_g} - \frac{1}{D_{iq}} \sqrt{\left(\frac{V_n}{N X_g}\right)^2 - i_d^2} \quad (23)$$

where N is the number of paralleled inverters in the PV power plant, and $i_d = I_d / N$ is approximated to the d -axis current of the individual inverter, which is readily available in the inverter itself.

Since the parameter of grid impedance X_g can be obtained from the Transmission System Operator (TSO), or estimated using the online impedance measurement method [32], the voltage variations at PCC caused by the active power can be dynamically compensated based on the adaptive control law of (22). Even if voltage variation cannot be perfectly compensated due to possible parameter mismatch, the inherent droop scheme will be effective to deal with the uncompensated voltage variation in the traditional way.

Therefore, the reactive power demands can be automatically dispatched on the individual inverters without deteriorating V_{pcc} , and the power transfer capacity of the PV power plant can be maximized.

Accordingly, the detailed control scheme of the individual PV inverter can be depicted by Fig. 10, where the current control is performed under the dq domain. The current reference in d axis is obtained by dividing the power command with the PCC voltage V_{pcc} , where the power command from the maximum power point tracking (MPPT) is replaced by the look up table to simulate the daily generation curve. The current reference in q axis is obtained by the proposed adaptive droop control that depicted by Fig. 9(b) and Eq (23).

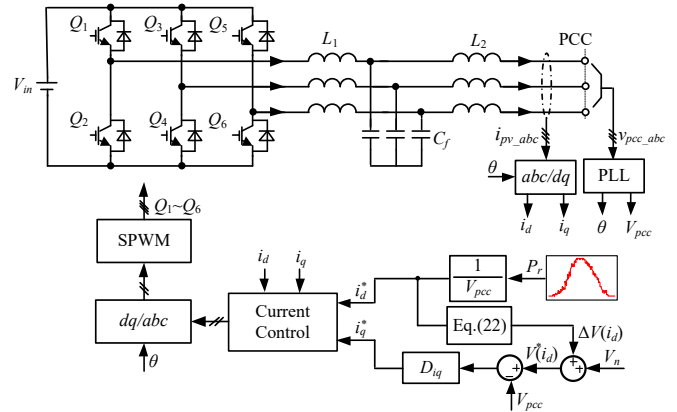


Fig. 10. Control scheme of the proposed adaptive reactive power control.

VI. SIMULATION AND EXPERIMENTAL VERIFICATION

A. Description of the PV power plant

In order to verify the effectiveness of theoretical analysis and the proposed adaptive reactive power control method, a simulation model of 200 MW PV power plant is built in PLECS. It contains $N=5000$ of PV inverters, and the key parameters of each inverter are shown in Table. 1.

TABLE I.
PARAMETERS OF EACH PV INVERTER IN A PV POWER PLANT

Symbol	Meaning	Value
V_g	Grid voltage (phase)	230 V
f_i	Grid frequency	50 Hz
P_n	Rated Output Power	40 kW
S_{max}	Maximum apparent power	44.44 kVA
PF	Power factor	-0.9~+0.9
I_n	Maximum current rating (RMS)	193.2 A

According to (11) and the PF limitation in Table I, the minimum SCR for the PV power plant to ensure rated power injection can be obtained as $SCR_{min}=1.254$. So the PV power plant is operated under the $SCR=1.25$ to test this limitation. Meanwhile, the conventional droop control with $\Delta V_{max}=10\%V_n$ is used for comparison.

B. Simulation Results

The daily generation curves using conventional droop control are shown in Fig. 11. To obtain a readable figure, 5000 inverters are divided into 10 groups, so each group has a maximum current rating of $I_{max}=500I_m=96.6kA$, and i_{group} in Fig. 11 denotes the output current of inverter groups. P_t and Q_t are the total output active and reactive power of the PV power plant, respectively. As seen, the V_{pcc} is reduced to 210V at peak hours between 11:00 and 12:30, so the actual power transfer capability of PV power plant is reduced because the larger current is needed to deliver the rated real power. As a result, the actual active power of PV power plant is limited at 187MW. With the proposed adaptive droop control, as shown in Fig 12, the voltage drop can be compensated dynamically under different output power levels. Therefore, more active power can be delivered given the same current rating I_{max} , and 200MW rated power can be approximately achieved.

Since the proposed method needs to estimate grid impedance X_g to adjust V^* , simulation results with $\pm 20\%$ estimation error of X_g are presented in order to examine its robustness. As seen in Figs. 13 and 14, due to the parameter mismatch, V^* can be less-adjusted or over-adjusted, and the voltage variation can be observed at PCC. Nevertheless, it still works much better than the conventional droop control in terms of voltage regulation and power transfer capacity.

To further demonstrate the feasibility of the proposed adaptive reactive power control, Figs. 15 and 16 present the generation curves of the adaptive droop control under the ordinary weak grid condition with $SCR=5$ and 10 . As seen, the proposed adaptive reactive power control method works well for different grid conditions.

B. Down-scaled Experimental Results

To further verify the adaptive droop control method, the down-scaled experiment is carried out. The experimental setup is shown in Fig. 17, where the ultra weak grid is realized by connecting the inductors with the grid simulator, and control algorithms of the two inverters are implemented in the dSPACE1007. The circuit parameters are shown in Table II, where the grid voltage is intentionally reduced to create the ultra grid condition with $SCR=1.25$.

The experimental waveforms using conventional droop control are shown in Fig. 18. The PCC voltage V_{pcc} is reduced to 0.92 p.u. during peak generation time, so the actual power of PV power plant P_t is limited to 0.95 p.u of the rated power and the grid current of the inverters I_{gt} has achieved its maximum. With the proposed adaptive droop control, as shown in Fig 19, the voltage drop can be compensated dynamically at different output power levels. Therefore, more active power can be delivered given the same current rating, and 1.0 p.u. rated power can be approximately achieved. Therefore, the experimental results match well with the simulation results, which further confirm the theoretical analysis and effectiveness of the proposed adaptive droop control method.

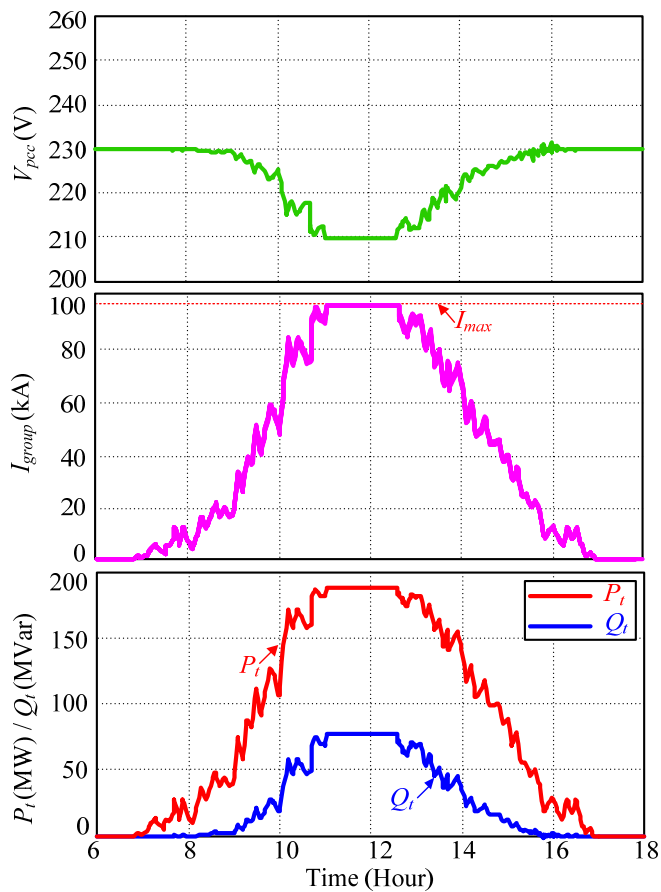


Fig. 11. Waveforms of V_{pcc} , I_{group} , P_t and Q_t using the conventional droop control.

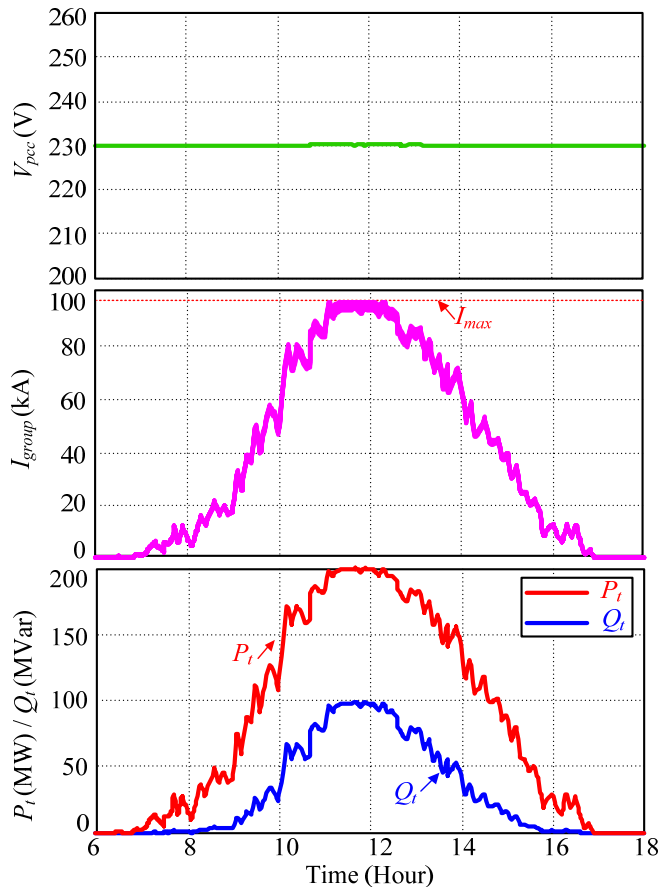


Fig. 12. Waveforms of V_{pcc} , I_{group} , P_t and Q_t using the proposed adaptive droop control without parameter mismatch.

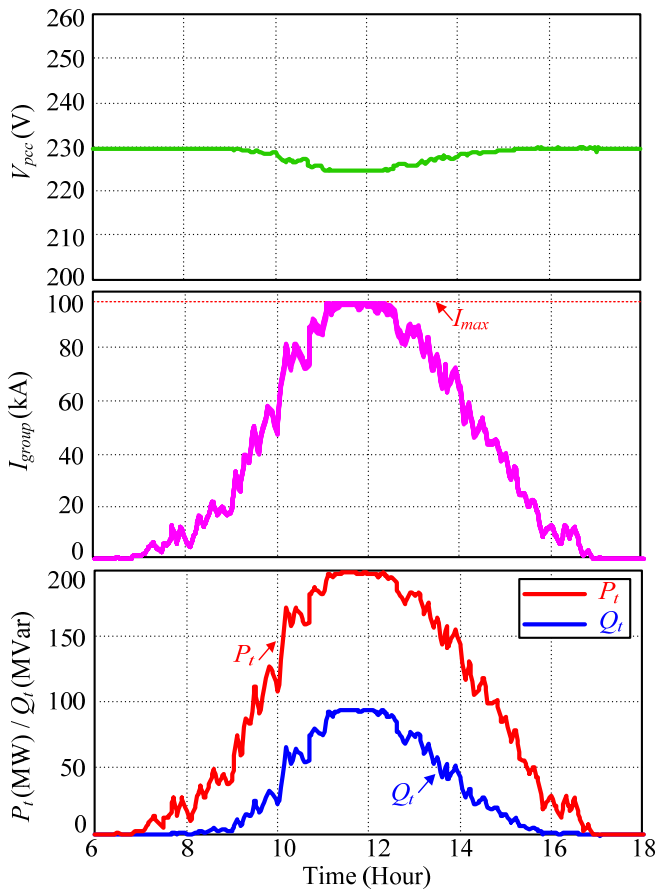


Fig. 13. Waveforms of V_{pcc} , I_{group} , P_t and Q_t using the proposed adaptive droop control with -20% parameter mismatch.

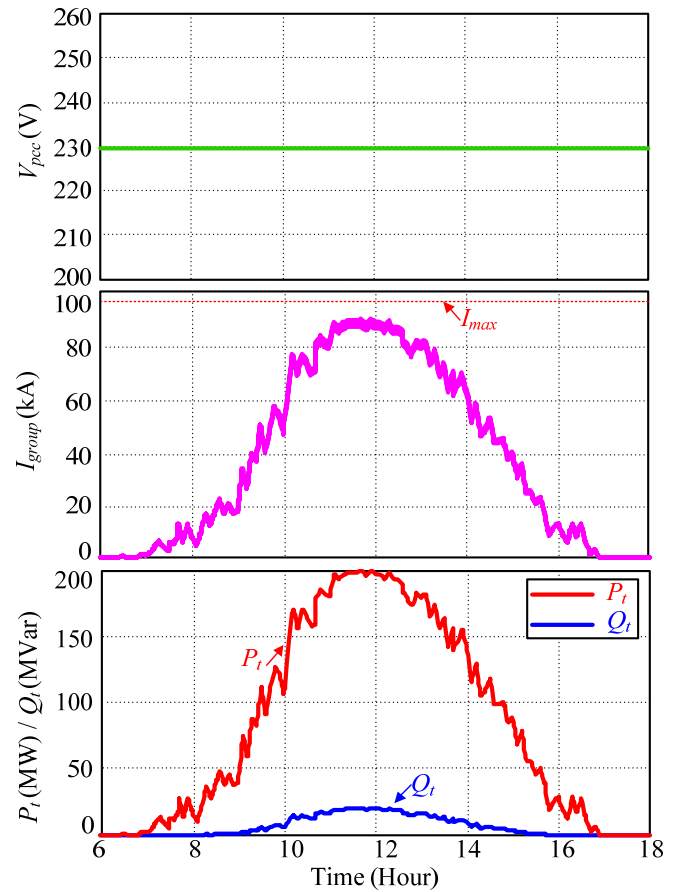


Fig. 15. Waveforms of V_{pcc} , I_{group} , P_t and Q_t using the proposed adaptive droop control under ordinary weak grid with $SCR=5$.

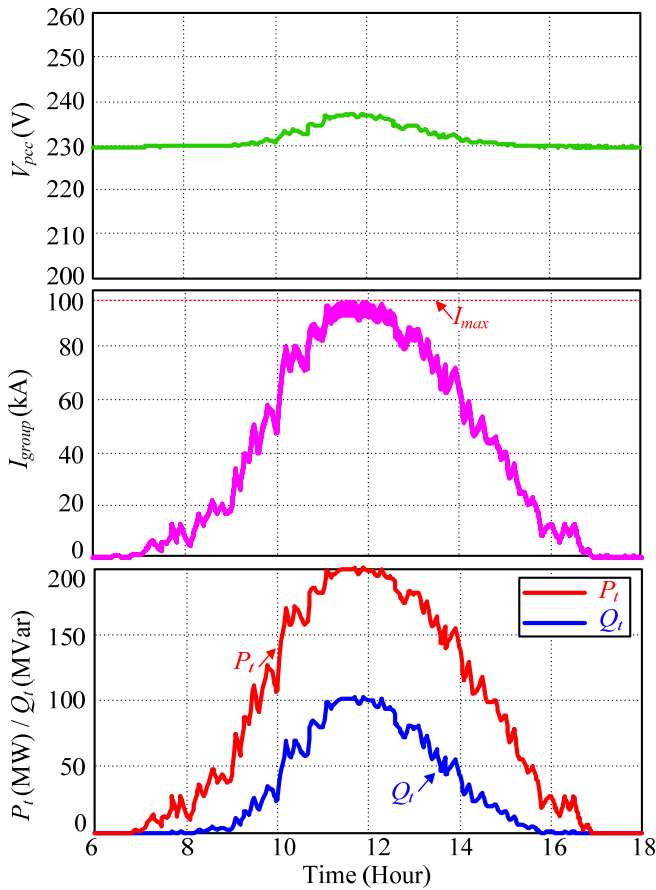


Fig. 14. Waveforms of V_{pcc} , I_{group} , P_t and Q_t using the proposed adaptive droop control with $+20\%$ parameter mismatch.

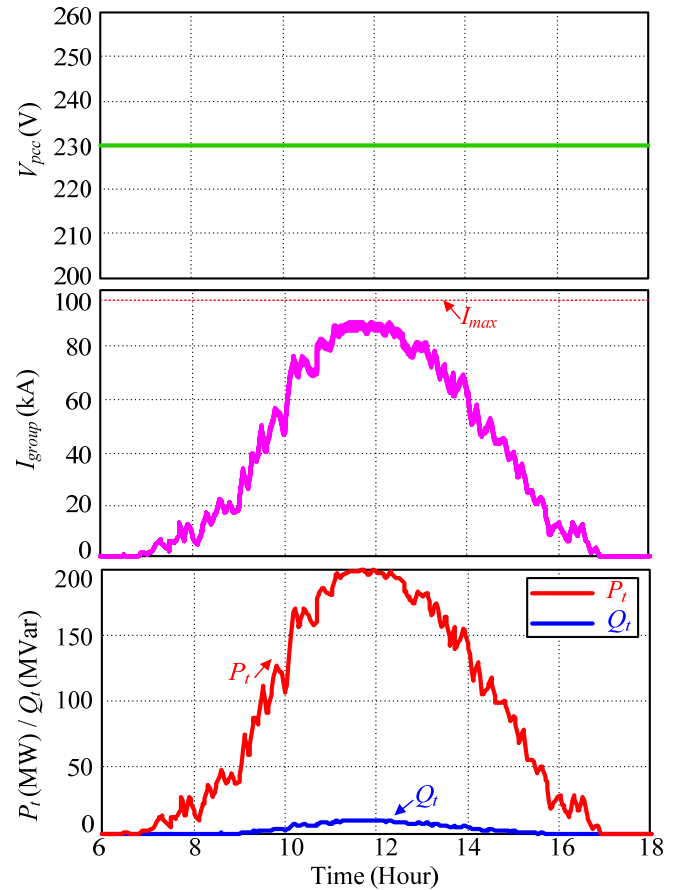


Fig. 16. Waveforms of V_{pcc} , I_{group} , P_t and Q_t using the proposed adaptive droop control under ordinary weak grid with $SCR=10$.

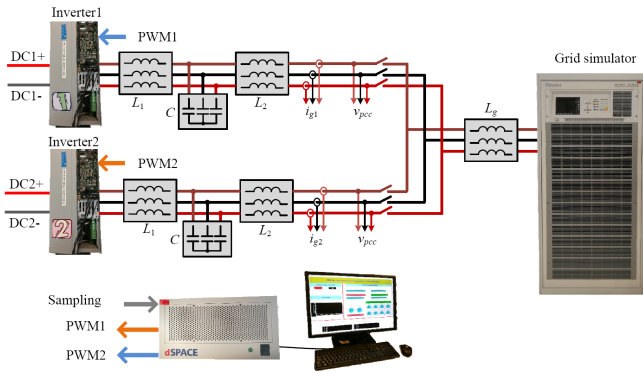


Fig. 17 Photo of the experimental setup.

TABLE II
PARAMETERS OF GRID CONNECTED INVERTER

Parameter	Values
V_{dc}	Input dc-link voltage 600 V
V_g	Phase grid voltage, peak value 80 V (1 p.u.)
f_0	Fundamental frequency 50 Hz
f_{sw}	Switching frequency 10 kHz
L_1	Inverter-side inductor 1.5mH
C	Filter capacitor 5 μ F
L_2	Grid-side inductor 1.5mH
L_g	Grid impedance 12.5mH (0.8 p.u.)
P_n	Rated Output Power 1 kW (1 p.u.)
S_{max}	Maximum apparent power 1.11 kVA (1.11 p.u.)
I_m	Maximum phase current, peak vlaue 9.26 A (1.11p.u.)
PF	Power factor -0.9~+0.9

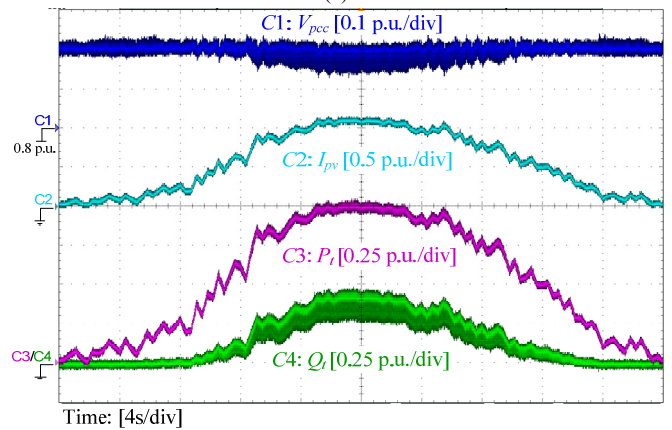
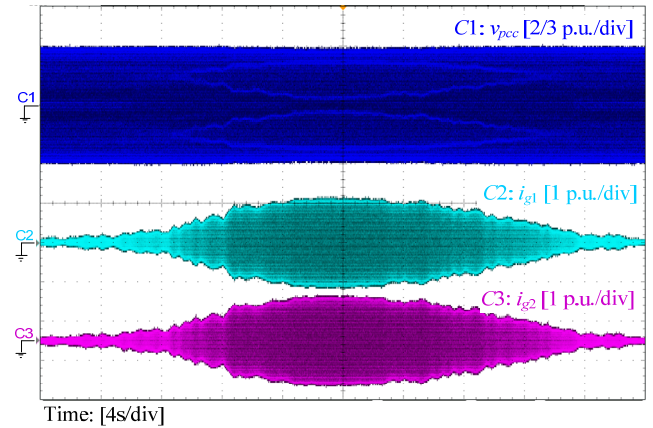


Fig. 19. Experimental waveforms using the proposed adaptive droop control.

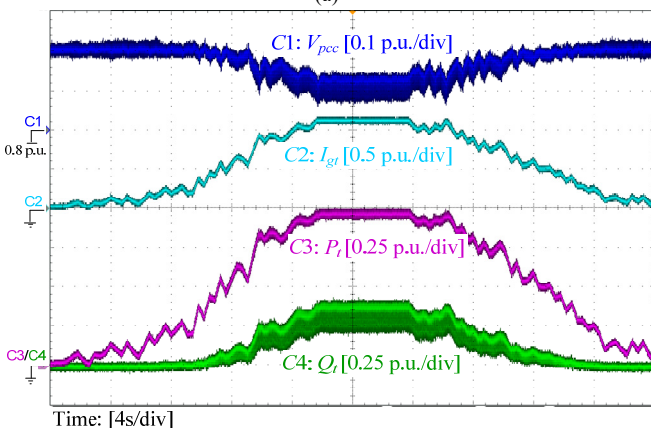
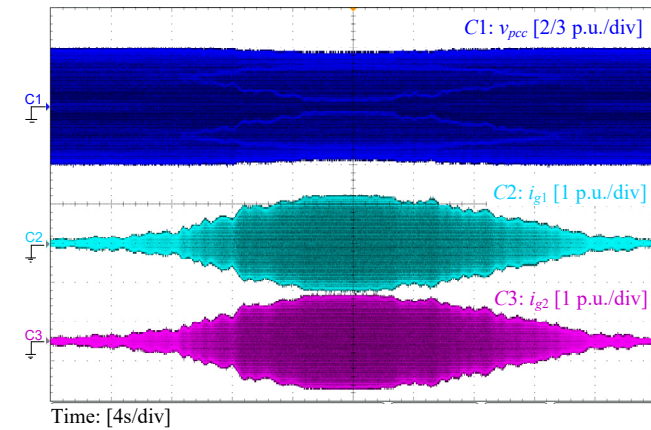


Fig. 18. Experimental waveforms using the conventional droop control.

VII. CONCLUSION

This paper investigates the power limitation of a PV power plant under ultra-weak grid condition with SCR close to 1. It is revealed that low R/X ratio of the transmission line will impose more severe power limitation on the PV power plant. A minimum SCR of 2 is required for the PV power plant to ensure the rated real power injection when it is operated with unity power factor. This requirement can be reduced when the inverters in the PV power plant can provide the reactive power compensation, and the minimum SCR with different PF is derived. Moreover, the optimized coordination of the active and reactive power is studied. It reveals that the power transfer capacity of PV power plant can be maximized by outputting the reactive power as much as possible until the PCC voltage achieves its limitation. Moreover, an adaptive reactive power droop control method is proposed which can improve the power transfer capacity of the PV power plant to its theoretical limitation under the ultra-weak grid condition with an SCR as low as 1.25.

REFERENCES

- [1] M. Campbell, P. Aschenbrenner, J. Blunden, E. Smeloff, S. Wright, "The drivers of the levelized cost of electricity for utility-scale photovoltaics," SunPower Corp., 2008.
- [2] F. Blaabjerg, Y. Yang, D. Yang, and X. Wang, "Distributed power-generation systems and protection," *Proc. IEEE*, vol. 105, no. 7, pp.1311-1331, Jul. 2017.
- [3] "Another record year for utility-scale solar takes cumulative capacity close to 100 GW," Wiki-solar, 2017.
- [4] "Energy from the desert: very large scale PV power plants for shifting to renewable energy future," International Energy Agency,

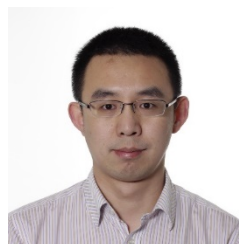
- 2015.
- [5] "Utility-scale solar photovoltaic power plants-A project developer's guide," International Finance Corporation (IFC), 2015.
- [6] T. Brown, "Transmission network loading in Europe with high shares of renewables," *IET Renewable Power Generation*, vol. 9, no. 1, pp.57-65, Jan. 2015.
- [7] N. Florentzou, V. G. Agelidis, and G. D. Demetriades, "VSC-based HVDC power transmission systems: An overview," *IEEE Trans. Power Electron.*, vol. 24, no. 3, pp. 592-602, Mar. 2009.
- [8] P. Rao, M. L. Crow, and Z. Yang, "STATCOM control for power system voltage control applications," *IEEE Trans. Power Del.*, vol. 15, pp. 1311-1317, Oct. 2000.
- [9] L. Xu, P. Dong, and M. Liu, "A comparative analysis of the interaction between different FACTS and HVDC," in *Proc. IEEE Power and Energy Society General Meeting*, 2012, pp. 1-5.
- [10] Y. Jiang, J. Sun, W. Hu, S. Li, H. Zhou, and X. Zha, "Analysis and suppression of interaction between STATCOM and voltage-source inverter in islanded micro-grid," in *Proc. IEEE Energy Conversion Congress and Exposition (ECCE)*, pp.6858-6863, 2015.
- [11] H. J. Kim, N. Taesik, H. Kyeon, C. Byunghoon, J. H. Chow, and R. Entriiken, "Dynamic interactions among multiple FACTS controllers, A survey," in *Proc. IEEE Power and Energy Society General Meeting*, 2011, pp. 1-8.
- [12] M. Amin, M. Molinas, "Understanding the origin of oscillatory phenomena observed between wind farms and HVDC systems," *IEEE J. Emerg. Sel. Topics Power Electron.*, vol. 5, no. 1, pp.378-392, Mar., 2017.
- [13] A. Moawwad, V. Khadkikar and J. Kirtley, "Photovoltaic power plant as FACTS devices in multi-feeder systems," in *Proc. 37th Annual Conference of the IEEE Industrial Electronics Society (IECON)*, pp. 918-923, 2011.
- [14] R. Varma, and R. Salehi, "SSR mitigation with a new control of PV solar farm as STATCOM (PV-STATCOM)" *IEEE Trans. Sustain. Energy*, 2017, vol. 8, pp. 1473-1483, Apr., 2017.
- [15] R. Varma, S. Rahman, and T. Vanderheide, "New control of PV solar farm as STATCOM (PV-STATCOM) for increasing grid power transmission limits during night and day," *IEEE Trans. Power Del.*, vol. 30, no. 2, pp. 755-763, Apr., 2015.
- [16] J. Zhou and A. Gole, "VSC transmission limitations imposed by AC system strength and AC impedance characteristics," in *Proc. 10th IET International Conference on AC and DC Power Transmission (ACDC)*, pp. 1-6, 2012.
- [17] *IEEE Std 929-2000*, IEEE Recommended practice for utility interface of photovoltaic (PV) systems, ISBN 0-7381- 1934-2 SH94811, 2000.
- [18] *GB/T19964-2012*. Photovoltaic power plant power system access technical requirements. Beijing: General Administration of Quality Supervision, Inspection and Quarantine of People's Republic of China, China National Standardization Management Committee, 2012.
- [19] G. Valverde and T. Van Cutsem, "Model predictive control of voltages in active distribution networks," *IEEE Trans. Smart Grid*, vol. 4, no. 4, pp. 2152-2161, Dec. 2013.
- [20] A. Gabash and P. Li, "Active-reactive optimal power flow for low-voltage networks with photovoltaic distributed generation," in *Proc. IEEE Int. Energy Conf. Exhibition, Florence*, pp. 381-386, 2012.
- [21] Y. He, M. Petit, and P. Dessante, "Optimization of the steady voltage profile in distribution systems by coordinating the controls of distributed generations," in *Proc. 3rd IEEE PES Innov. Smart Grid Technol*, pp. 1-7, 2012.
- [22] S. Bolognani and S. Zampieri, "A distributed control strategy for reactive power compensation in smart microgrids," *IEEE Trans. Autom. Control*, vol. 58, no. 11, pp. 2818-2833, Nov. 2013.
- [23] P. Carvalho, P. Correia, and L. Ferreira, "Distributed reactive power generation control for voltage rise mitigation in distribution networks," *IEEE Trans. Power Syst.*, vol. 23, no. 2, pp. 766-772, May 2008.
- [24] G. Mokhtari, A. Ghosh, G. Nourbakhsh, and G. Ledwich, "Smart robust resources control in LV network to deal with voltage rise issue," *IEEE Trans. Sustain. Energy*, vol. 4, no. 4, pp. 1043-1050, Oct. 2013.
- [25] L. Collins and J. Ward, "Real and reactive power control of distributed PV inverters for overvoltage prevention and increased renewable generation hosting capacity," *Renewable Energy*, vol. 81, pp. 464-471, 2015.
- [26] K. Turitsyn, P. Sulc, S. Backhaus, and M. Chertkov, "Options for control of reactive power by distributed photovoltaic generators," *Proc. IEEE*, vol. 99, no. 6, pp. 1063-1073, Jun. 2011.
- [27] E. Demirok, P. Casado Gonzalez, K. H. Frederiksen, D. Sera, P. Rodriguez, and R. Teodorescu, "Local reactive power control methods for overvoltage prevention of distributed solar inverters in low-voltage grids," *IEEE J. Photovolt.*, vol. 1, no. 2, pp. 174-182,

Oct. 2011.

- [28] E. Demirok, "Control of grid interactive PV inverters for high penetration in low voltage distribution networks," Ph.D. dissertation, Dept. Energy Technology, Univ. Aalborg, 2012.
- [29] S. Weckx, J. Driesen, "Optimal local reactive power control by PV inverters," *IEEE Transactions on Sustainable Energy*, vol 7, pp.1624-1633, Oct. 2016.
- [30] G. Fusco, Mario Russo, "Robust MIMO design of decentralized voltage controllers of PV systems in distribution networks," *IEEE Trans. Ind. Electron.*, vol. 64, no. 6, pp. 4610-4620, Jan., 2017.
- [31] Á. Molina-García, R. A. Mastromauro, T. García-Sánchez, S. Pugliese, M. Liserre, S. Stasi, "Reactive power flow control for PV inverters voltage support in LV distribution networks," *IEEE Trans. Smart Grid*, vol. 8, no. 1, pp. 447-456, Jan. 2017.
- [32] A. V. Timbus, R. Teodorescu, and U. Borup, "Online grid impedance measurement suitable for multiple PV inverters running in parallel," in *Proc. IEEE 21st Annu. Appl. Power Electron. Conf.*, pp. 907-911, 2006.



Dongsheng Yang (S'13-M'17) was born in Jiangsu Province, China, in 1984. He received the B.S., M.S., and Ph.D. degrees in electrical engineering from Nanjing University of Aeronautics and Astronautics, Nanjing, China, in 2008, 2011, and 2016, respectively. Since 2016, he has been with Aalborg University, Aalborg, Denmark, where he is currently a Postdoctoral Researcher in the Department of Energy Technology. His main research interests include design and control of grid-connected inverters, harmonic analysis and mitigation in power-electronic-based power systems, and online impedance measurement techniques.



Xiongfei Wang (S'10-M'13-SM'17) received the B.S. degree from Yanshan University, Qinhuangdao, China, in 2006, the M.S. degree from Harbin Institute of Technology, Harbin, China, in 2008, both in electrical engineering, and the Ph.D. degree in energy technology from Aalborg University, Aalborg, Denmark, in 2013. Since 2009, he has been with the Aalborg University, Aalborg, Denmark, where he is currently an Associate Professor in the Department of Energy Technology. His research interests include modeling and control of grid-connected converters, harmonics analysis and control, passive and active filters, stability of power electronic based power systems.

Dr. Wang serves as an Associate Editor for the IEEE TRANSACTIONS ON POWER ELECTRONICS, the IEEE TRANSACTIONS ON INDUSTRY APPLICATIONS, and the IEEE JOURNAL OF EMERGING AND SELECTED TOPICS IN POWER ELECTRONICS. He is also the Guest Editor for the Special Issue "Grid-Connected Power Electronics Systems: Stability, Power Quality, and Protection" in the IEEE TRANSACTIONS ON INDUSTRY APPLICATIONS. He received the second prize paper award and the outstanding reviewer award of IEEE TRANSACTIONS ON POWER ELECTRONICS in 2014 and 2017, respectively, the second prize paper award at IEEE IAS-IPCC in 2017, and the best paper awards at IEEE PEDG 2016 and IEEE PES GM 2017.

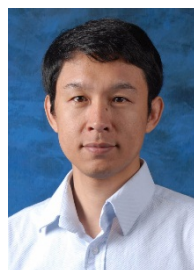


Fangcheng Liu received the B.S. degree from Huazhong University of Science and Technology, Wuhan, China, in 2007, the Ph.D. degree from Xi'an Jiaotong University, Xi'an, China, in 2014, both in electrical engineering. Since 2014, he has been with Huawei, where he is currently a researcher at Watt Lab (Part of Central Research Institute). His main research interests include modeling and control of grid-connected converters, and stability of power electronic based power systems.



Kai Xin received the Ph.D. degree in electrical engineering from Huazhong University of Science and Technology, Wuhan, China in 2007. He was a Researcher at Power Conversion System Control Lab in General Electric Global Research Center, Shanghai, China, from 2007 to 2011. Since 2011, he has been with Huawei, where he is currently a Technical Expert of Network Energy Product Line and Project Leader of Watt Lab (Part of Central Research Institute). His main research interests include Grid-connected PV/wind power generation

system, and Energy conversion techniques and applications.



Yunfeng Liu received the Ph.D degree in electronic engineering from Southeast University, Nanjing, China, in 1999. He was a Postdoctoral Researcher in the Department of Electrical Engineering of Tsinghua University, Beijing, China, from 1999 to 2001. He was a Visiting Scholar at Virginia Tech-CPES, Virginia, US, from 2001 to 2003. He was the Senior Researcher at General Electric Global Research Center (GE GRC), Shanghai, China and later as Manager of Power Conversion System Control Lab of GE GRC, from 2003 to 2011. Since 2011, he has been with Huawei,

where he is currently the Chief Scientist of Network Energy Product Line and Manager of Watt Lab (Part of Central Research Institute). His main research interests include High power semiconductor devices, converter and application in power system, and Energy conversion techniques and applications.



Frede Blaabjerg (S'86–M'88–SM'97–F'03) received the Ph.D. degree in electrical engineering from Aalborg University, Aalborg, Denmark, in 1995. He was with ABB-Scandia, Randers, Denmark, from 1987 to 1988. He became an Assistant Professor in 1992, an Associate Professor in 1996, and a Full Professor of power electronics and drives in 1998 at Aalborg University. In 2017, he became the Doctor Honoris Causa at the University of Politehnica, Timisoara, Romania.

His current research interests include power electronics and its applications such as in wind turbines, PV systems, reliability engineering, power quality, and adjustable speed drives. Prof. Blaabjerg has received 18 IEEE Prize Paper Awards, the IEEE PELS Distinguished Service Award in 2009, the EPE-PEMC Council Award in 2010, the IEEE William E. Newell Power Electronics Award 2014 as well as the Villum Kann Rasmussen Research Award 2014. He was the Editor-in-Chief of the IEEE TRANSACTIONS ON POWER ELECTRONICS from 2006 to 2012. He was nominated by Thomson Reuters as one of the 250 most cited researchers in engineering in the world in 2014, 2015, and 2016.